Vocal Fold Collision Modeling

Granados, Alba; Brunskog, Jonas; Misztal, M. K.

Published in:
Proceedings of the 9th International Workshop on Models and Analysis of Vocal Emissions for Biomedical Application

Publication date:
2015

Document Version
Peer reviewed version

VOCAL FOLD COLLISION MODELING

A. Granados[1], J. Brunskog[1] , M. K. Misztal[2]

[1] Acoustic Technology, Technical University of Denmark, Kongens Lyngby DK-2800, Denmark
[2] Niels Bohr Institute, University of Copenhagen, Copenhagen DK-2100, Denmark
algra@elektro.dtu.dk

Abstract: **When vocal folds vibrate at normal speaking frequencies, collisions occurs. The numerics and formulations behind a position-based continuum model of contact is an active field of research in the contact mechanics community. In this paper, a frictionless three-dimensional finite element model of the vocal fold collision is proposed, which incorporates different procedures used in contact mechanics and mathematical optimization theories. The penalty approach and the Lagrange multiplier method are investigated. The contact force solution obtained by the penalty formulation is highly dependent on the penalty parameter value. Furthermore, the Lagrange approach shows poor results with regard to instantaneous contact force estimation. This motivates the use of an Augmented Lagrange approach to regularize the Lagrange contact force solution. Finally, the effect of the interpenetration volume on contact force and contact area computations is illustrated.**

Keywords : **Vocal folds, collision, constrained optimization, finite element method, contact detection.**

I. INTRODUCTION

Mathematical descriptions of self-oscillating finite element models of the vocal folds have been reported in the literature (e.g., see [1]). A continuum model of the airflow coupled to a deformable three-dimensional body have been one of the main focuses. For purpose of clinical research, investigations on the mechanical conditions that arise during phonation are of special interest. At normal speaking frequencies, vocal fold collision occurs, and the tissue is affected by specific stresses and reaction forces [2]. Hence, a detailed mathematical study of the collision process is expected to contribute to a better understanding of vocal fold mechanics.

In the context of continuum mechanics, the vocal fold contact can be modeled by enforcing position-based constraints to the minimization of the total potential energy of the mechanical system. Methodologies from mathematical optimization theory can be applied in order to solve the contact constrained problem [3]. In this paper, a Penalty method and a Lagrange multiplier approach are investigated for the the case of frictionless vocal fold collision. Furthermore, a penalty regularization of the Lagrange multiplier method is carried out by the Augmented Lagrange technique applied together with an Uzawa type algorithm [3]. Finite element contact discretization and contact detection mechanism that allows for asymmetric collision are presented.

II. METHODOLOGY

A three-dimensional deformable viscoelastic model of the vocal folds driven by a Bernoulli glottal airflow is described. At each time step the new equilibrium position is found as the minimum of the total potential energy by the variational formulation. When collision occurs, the contact constrained minimization problem is solved by different methods.

A. Governing equations

In the absence of volume forces, the vocal fold deformation is described by the equation of balance

$$\nabla \cdot \boldsymbol{\sigma} = \rho \frac{\partial^2 \boldsymbol{x}}{\partial t^2} \qquad \boldsymbol{x} \in v_{\text{solid}}, \tag{1}$$

in the deformed state $v_{\text{solid}} \subset \mathbb{R}^3$, the constitutive equation for a transversely isotropic linear viscoelastic solid as in [4], and the Dirichlet and Neumann boundary conditions

$$\boldsymbol{x} - \boldsymbol{X} = 0 \qquad \text{in } \Gamma_D \subset \partial v_{\text{solid}} \tag{2.1}$$

$$\boldsymbol{\sigma} \cdot \boldsymbol{n} = \boldsymbol{p} \qquad \text{on } \Gamma_N \subset \partial v_{\text{solid}} \tag{2.2}$$

respectively, where $\boldsymbol{\sigma}$ is the stress tensor, $\boldsymbol{X}$ represents the material coordinates, $\boldsymbol{n}$ is the outward normal, and $\boldsymbol{p}$ is the aerodynamic pressure derived from Bernoulli's principle. The Dirichlet boundary where the displacement is zero is placed in the anteroposterior glottal regions; see [3] for further details. The equilibrium position can be found as the minimum of the total potential energy Π . Hence, for

admissible displacement variations or test functions $\boldsymbol{w}$ that vanish in the Dirichlet boundary, the weak formulation of the problem takes the form

$$\delta\Pi=\int_{v_{solid}}\rho\,\boldsymbol{w}^t\cdot\frac{\partial^2\boldsymbol{x}}{\partial t^2}\,\mathrm{d}v+\int_{v_{solid}}\nabla\boldsymbol{w}^t:\boldsymbol{\sigma}\,\mathrm{d}v-\int_{\Gamma_N}\boldsymbol{w}^t\cdot\boldsymbol{p}\,\mathrm{d}\Gamma=0, \quad (3)$$

where $\delta\Pi$ indicates the variation of the energy.

When collision between the vocal folds occurs, additional constraints may be activated on the contact area $\Gamma_C\subset\partial v_{solid}$. In order to avoid unphysical body interpenetration for a frictionless contact, non-negativeness of the normal gap between a superficial slave node $\boldsymbol{x}^s$ and a master surface placed at the opposite vocal fold may be enforced by the position-based constraint

$$g_N=\left(\boldsymbol{x}^s-\overline{\boldsymbol{x}}^m\right)\cdot\overline{\boldsymbol{n}}^m\geq 0 \qquad \text{on } \Gamma_C\subset\partial v_{\text{solid}}, \quad (4)$$

where $\overline{\boldsymbol{x}}$ is the projection of the slave node onto the master surface; see Fig. 1.

B. Contact constraint enforcement

A penalty, a Lagrangian and an augmented Lagrangian [3] methods are here studied to enforce the inequality constraint in Eq. (4). Only the Lagrangian solution enforces the collision constraint in exact form.

The penalty method consists of a minimization problem where the objective function involves the collision-free potential energy and a term which penalizes infeasible positions on Γ_C as

$$\Pi+\int_{\Gamma_c}\frac{1}{2}\kappa\left|g_N(\boldsymbol{x})\right|^2\mathrm{d}\Gamma, \quad (5)$$

where $\kappa>0$ is a penalty parameter. Optimality conditions lead to the variational formulation

$$\delta\Pi+\int_{\Gamma_C}\kappa\left(\boldsymbol{w}^s-\overline{\boldsymbol{w}}^m\right)\cdot\left(\boldsymbol{x}^s-\overline{\boldsymbol{x}}^m\right)\mathrm{d}\Gamma=0 \quad (6)$$

to be combined with Eq. (3). The second term above can be interpreted as minus the reaction force to avoid interpenetration. For non-adhesion contact, the reaction force must be compressive. Hence, it can be seen that as the penalty parameter tends to infinity the normal gap tends to zero, and the optimal of the new minimization problem approaches the exact equilibrium solution at collision. However, large penalty parameters may lead to ill-conditioning of the global matrix.

The Lagrangian method solves the inequality constrained problem by solving the optimization problem with objective function

$$L(\boldsymbol{x},\boldsymbol{\Lambda})=\Pi+\int_{\Gamma_c}\boldsymbol{\Lambda}\,g_N(\boldsymbol{x})\,\mathrm{d}\Gamma, \quad (7)$$

called the Lagrangian function, where $\boldsymbol{\Lambda}$ is the Lagrange multiplier vector, also called dual variables. Optimality conditions to the problem are

$$\delta\Pi+\int_{\Gamma_C}\boldsymbol{\Lambda}\left(\boldsymbol{w}^s-\overline{\boldsymbol{w}}^m\right)\cdot\overline{\boldsymbol{n}}^m\,\mathrm{d}\Gamma=0$$
$$\boldsymbol{\Lambda}\leq 0$$
$$\boldsymbol{\Lambda}\cdot g_N(\boldsymbol{x})=0, \quad (8)$$

which are known as the Karush-Kuhn-Tucker conditions for optimality. Note that the Lagrange multiplier vector can be seen as the compressive reaction forces. From a physical point of view, the last condition indicates that no contact forces are active when the normal gap is positive, and the non-penetration constraint is fulfilled in exact form whenever collision occurs. However, this approach introduces additional unknowns in the form of Lagrange multipliers. Furthermore, the Lagrangian approach in Eq. (8) is a non-smooth contact formulation, and regularization techniques may be used to improve results.

The Augmented Lagrange formulation combines the Lagrange and the penalty approaches, without additional unknowns. A simplified version is the Uzawa algorithm [3] which may be summarized as follows. For an initial Lagrange multiplier vector $\boldsymbol{\Lambda}_k$, a new equilibrium is found by minimization of

$$\Pi+\int_{\Gamma_c}\boldsymbol{\Lambda}_k\,g_N(\boldsymbol{x})\,\mathrm{d}\Gamma+\int_{\Gamma_c}\frac{1}{2}\kappa\left|g_N(\boldsymbol{x})\right|^2\mathrm{d}\Gamma, \quad (9)$$

where the last penalty term can be seen as a regularization term for non-smoothness. The Lagrange multiplier vector is updated in an augmentation iteration as

$$\boldsymbol{\Lambda}_{k+1}=\boldsymbol{\Lambda}_k+\min\left\{\kappa\,g_N(\boldsymbol{x}_{k+1}),\boldsymbol{\Lambda}_k\right\}, \quad (10)$$

where $\boldsymbol{x}_{k+1}$ is the solution of the minimization problem. The update in Eq. (10) can be seen as a gradient ascent algorithm, as the critical point of the Lagrangian in Eq. (7) occurs at a maximum over the multipliers [5]. As the contact constraint is not solved in an exact form, the augmentation procedure in Eq. (10) continues until a convergence criterion for $g_N(\boldsymbol{x}_{k+1})$ is fulfilled. Furthermore, the penalty parameter can be increased at each augmentation step to speed up the convergence rate. However, to avoid ill-conditioning of the system matrix due to a large

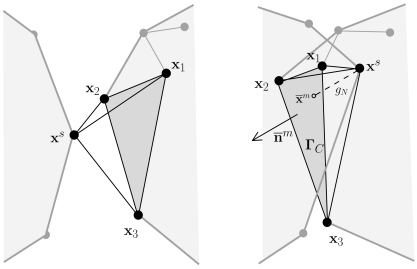

FIG. 1. Conforming interface mesh for collision detection; before (left) and after collision (right).

penalty parameter value, a maximum number of augmentations must be requested.

C. Spatial and temporal discretization

The spatial finite element discretization is based on a tetrahedral mesh. Hence, the interface domain is formed by triangular elements. As Fig. 1 illustrates, a coarse conforming interface tetrahedral mesh may be defined to detect contact; whenever an oriented interface element volume is inverted, collision occurs. Once the slave node $\boldsymbol{x}^s$ and the master surface with vertices $\boldsymbol{x}_1$, $\boldsymbol{x}_2$ and $\boldsymbol{x}_3$ are detected, by means of an isoparameteric transformation with linear basis functions $N_i(\xi,\zeta)$ defined on a reference triangular element, the projection $\overline{\boldsymbol{x}}^m$ corresponds to the local coordinates $(\overline{\xi},\overline{\zeta})$, and a contact element matrix

$$\boldsymbol{g}^e=\left(\overline{\boldsymbol{n}}^m-N_1(\overline{\xi},\overline{\zeta})\overline{\boldsymbol{n}}^m-N_2(\overline{\xi},\overline{\zeta})\overline{\boldsymbol{n}}^m-N_3(\overline{\xi},\overline{\zeta})\overline{\boldsymbol{n}}^m\right) \quad (11)$$

with $\boldsymbol{g}^e\cdot(\boldsymbol{x}^s\ \boldsymbol{x}_1\ \boldsymbol{x}_2\ \boldsymbol{x}_3)\geq 0$ contributes to the assembled global constraint contact matrix $\boldsymbol{G}$.

The penalty approach in Eq. (6) can be simplified further in the way that follows. Once a negative oriented element volume V^e is found, the compressive reaction force on a colliding element may be approximated numerically as

$$-(\boldsymbol{g}^e)^t\kappa\,\boldsymbol{g}^e\cdot(\boldsymbol{x}^s\ \boldsymbol{x}_1\ \boldsymbol{x}_2\ \boldsymbol{x}_3)^t\approx\overline{\boldsymbol{n}}^m(-1\ \ 1\ \ 1\ \ 1)^t\frac{\kappa V^e}{4} \quad (12)$$

Hence, a matrix $\boldsymbol{F}_c$ can be assembled. For global mass, damping, and stiffness matrices $\boldsymbol{M}$, $\boldsymbol{C}$, and $\boldsymbol{K}$, respectively, and $\boldsymbol{F}$ a vector of applied aerodynamic forces, the finite element system of the penalty approach is

$$\boldsymbol{M}\ddot{\boldsymbol{x}}+\boldsymbol{C}\dot{\boldsymbol{x}}+\boldsymbol{K}(\boldsymbol{x}-\boldsymbol{X})=\boldsymbol{F}+\boldsymbol{F}_c \quad (13)$$

The optimality condition for a Lagrangian approach in Eq. (9) consists of the equations

$$\begin{aligned}\boldsymbol{M}\ddot{\boldsymbol{x}}+\boldsymbol{C}\dot{\boldsymbol{x}}+\boldsymbol{K}(\boldsymbol{x}-\boldsymbol{X})+\boldsymbol{G}^t\boldsymbol{\Lambda}&=\boldsymbol{F}\\ \boldsymbol{G}\boldsymbol{x}&=\boldsymbol{0}\end{aligned} \quad (14)$$

When the second condition in Eq. (8) is not satisfied for all contact elements, the contact constraint is no longer, and a collision-free finite element system must be solved. The finite element discretization of the variation of the Augmented Lagrange formulation in Eq. (9) yields

$$\begin{aligned}\boldsymbol{M}\ddot{\boldsymbol{x}}_{k+1}+\boldsymbol{C}\dot{\boldsymbol{x}}_{k+1}+\boldsymbol{K}(\boldsymbol{x}_{k+1}-\boldsymbol{X})+\boldsymbol{G}^t\boldsymbol{\Lambda}_k\\ +\kappa(\boldsymbol{G}^t\boldsymbol{G}\,\boldsymbol{x}_{k+1})=\boldsymbol{F},\end{aligned} \quad (15)$$

where use is made of Eq. (14) and Eq. (6).

The temporal discretization scheme implemented for calculations is the Hilbert-Hughes-Tavlor $\alpha-$method. The parameters employed are $\alpha=-0.3$ and a time step increment $h=50\ \mu s$. These values give good accuracy and introduce advantageous numerical damping. Further details can be found in [4].

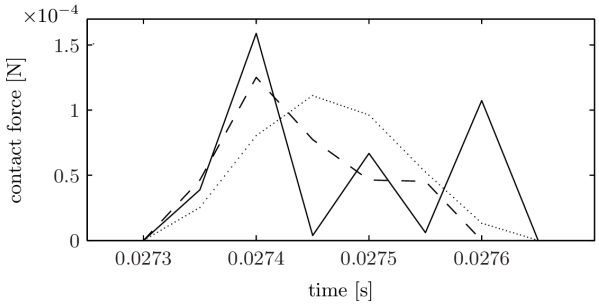

FIG. 2. Mediolateral coordinate of the contact force applied to an interface node. Solid line indicates the results for a Lagrange formulation; dotted line indicates the results for a penalty formulation with $\kappa=10^7$; dashed line indicates an Augmented Lagrangian formulation with 4 augmentations.

III. Results and Discussion

For all simulation, the tissue, geometry and initial conditions can be found in [4]. With regard to the augmented Lagrange technique, augmentations of a Lagrange multiplier associated to a slave node stop when the corresponding normal gap is less than 10^{-5}. The initial Lagrange multiplier vector is set to zero. The initial penalty parameter is 1, which increases by a factor of 10 when the total intersection volume is reduced by less than a 75% at each augmentation step.

The performance of different methods for contact constraint enforcement with regard to contact force estimations is illustrated in Fig. 2. The mediolateral component of the contact force applied to the interface node at initial position $(0.024,-0.136,-0.037)$ as a function of time is shown, for a subglottal pressure of 0.8 kPa. The results obtained by a penalty method with $\kappa=10^7$ are shown in dotted line; the Lagrange multiplier method, in solid line; the Augmented Lagrange formulation with a maximum of 4 augmentations, in dashed line. Comparison between the penalty and Lagrange reaction force solution, makes apparent a spurious non-smooth behavior of the Lagrange multiplier solution. From physical considerations, a smooth transition at each time step may be expected. Consequently, the Lagrange approach may lead to wrong estimations of the instantaneous contact force. In an effort to improve this unsatisfactory behavior, the Augmented Lagrange approach seems to have a regularization effect with 4 augmentations per time step.

Fig. 3 shows the maximum mediolateral component of the total contact force calculated from the summation over all nodal contact forces. Circles

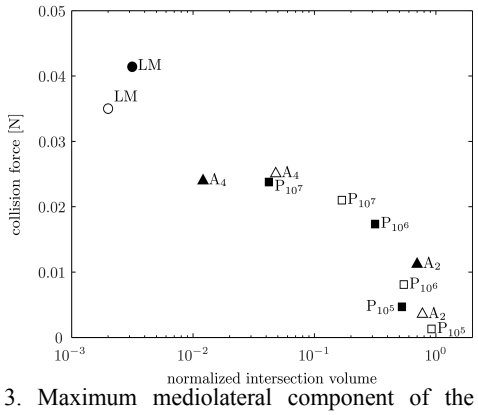

FIG. 3. Maximum mediolateral component of the total contact force as a function of the normalized intersection volume. The selected collision time interval is [0.036, 0.037], and the right vocal fold (x > 0) has been used for calculations.

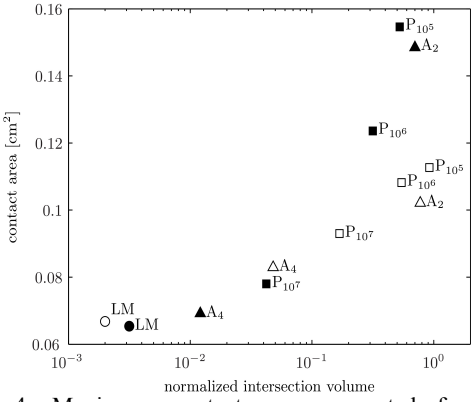

FIG. 4. Maximum contact area computed from the summation of interface triangles with any vertex loaded by a collision force. Symbols are the same as in Fig. 3.

indicate results for the Lagrange multiplier method (LM); squares correspond to a penalty formulation (P), where the subscript corresponds to the value of the penalty parameter; triangles correspond to the Augmented Lagrange approach (A), where the subscript indicates the maximum number of augmentations. Black and white marks show the results for a subglottal pressures of 0.8 kPa and 0.6 kPa, respectively. The horizontal axis corresponds to the interpenetration volume normalized to the maximum intersection volume when the effect of contact forces is neglected. The graph shows a clear effect of the violation of position-based contact constraint on contact force estimations. The Lagrange approach gives the smallest intersection volume, although, theoretically, the intersection volume should be zero. This small error is probably due to the contact detection algorithm. Furthermore, contact force computations with a penalty approach are highly dependent on the value of the penalty parameter. When the subglottal pressure is modified, the Lagrange approach shows robustness in comparison with the penalty results. With regard to the Augmented Lagrange procedure, ideally the augmented multipliers are not dependent on the penalty parameter [3]. However, the numerical solution behaves differently, which may be due to the contact finite element computations. Robustness in the method may be introduced by enlarging the maximum number of augmentations. Nevertheless, exact contact force solution cannot be assured as the penalty parameter tends to infinity, and ill-conditioning of the system matrix may occur.

Fig. 4 shows the maximum contact area computed from the summation of interface triangles with any vertex loaded by a collision force. An influence of the interpenetration volume is apparent from the results. Again, the Lagrange multiplier method seems to be robust for subglottal pressure variations.

IV. Conclusions

Position-based contact constraints of vocal fold collision have been shown to have a clear effect on collision force and contact area estimations. The Lagrange multiplier method for contact constraint enforcement appears to be robust for pressure variations, but poor with regard to instantaneous contact force solution. An Augmented Lagrange approach with an Uzawa algorithm has a smoothing effect by introducing a penalty regularization term. However, the Penalty and the Augmented Lagrange results show strong dependency on penalty parameter choice. Alternative formulations of contact constraint may further improve contact force estimations.

REFERENCES

[1] F. Alipour, D. A. Berry, and I. R. Titze, “A finite-element model of vocal-fold vibration.”, *J. Acoust. Soc. Am.* , vol. 108, pp. 3003–3012, 2000.

[2] H. E. Gunter, “A mechanical model of vocal-fold collision with high spatial and temporal resolution,” *J. Acoust. Soc. Am.*, vol. 113, pp. 994–1000, 2003.

[3] P. Wriggers, *Computational contact mechanics*, John Wiley & Sons, 2002.

[4] A. Granados, J. Brunskog , M. K. Misztal , V. Visseq, and K. Erleben “Finite element modeling of the vocal folds with deformable interface tracking,” in *Proc. Forum Acust.* (Krakow, Poland), 2014.

[5] N. Andreasson, and A. Evgrafov, and M. Patriksson, *Introduction to Continuous Optimization: Foundations and Fundamental Algorithms,* Studentlitteratur AB, 2006.